AD-A162 103 AN INTERPRETATION OF THE N2 PHOTOELECTRON SPECTRUM(U) 1/1
GEORGE WASHINGTON UNIV WASHINGTON D C DEPT OF CHEMISTRY
H SAMBE ET AL. OCT 85 TR-21 N00014-80-K-0852

UNCLASSIFIED F/G 7/4 NL

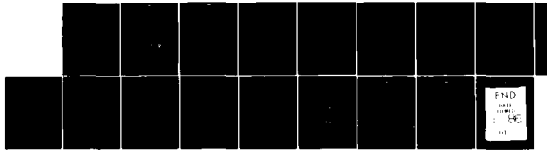

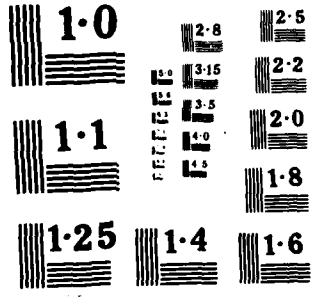
1·0
1·1
1·25
1·4
1·6
2·8
3·15
3·5
4·0
4·5
2·5
2·2
2·0
1·8

Unclassified

SECURITY CLASSIFICATION OF THIS PAGE (When Data Entered)

REPORT DOCUMENTATION PAGE	READ INSTRUCTIONS BEFORE COMPLETING FORM
1 REPORT NUMBER: No. 21 — 2 GOVT ACCESSION NO — 3 RECIPIENT'S CATALOG NUMBER	
4 TITLE (and Subtitle): AN INTERPRETATION OF THE N_2 PHOTOELECTRON SPECTRUM	5 TYPE OF REPORT & PERIOD COVERED: Technical Report
	6 PERFORMING ORG. REPORT NUMBER
7 AUTHOR(s): Hideo Sambe and David E. Ramaker	8 CONTRACT OR GRANT NUMBER(s): N00014-80-K-0852
9 PERFORMING ORGANIZATION NAME AND ADDRESS: Chemistry Department, George Washington University, Washington, D.C. 20052	10 PROGRAM ELEMENT, PROJECT, TASK AREA & WORK UNIT NUMBERS: Prog. Elem. No. 61153N, Task Area No. PP 013-08-01, Work Unit # NR 056-681
11 CONTROLLING OFFICE NAME AND ADDRESS: Office of Naval Research, Dept. of Navy, 800 N. Quincy Street, Washington, D.C. 22217	12 REPORT DATE: Oct. 1985
	13 NUMBER OF PAGES: 15
14 MONITORING AGENCY NAME & ADDRESS(if different from Controlling Office)	15 SECURITY CLASS (of this report): Unclassified
	15a DECLASSIFICATION/DOWNGRADING SCHEDULE

16 DISTRIBUTION STATEMENT (of this Report)

This document has been approved for public release and sale; its distribution is unlimited.

17 DISTRIBUTION STATEMENT (of the abstract entered in Block 20, if different from Report)

18 SUPPLEMENTARY NOTES

Submitted for publication in Chemical Physics Letters.

19 KEY WORDS (Continue on reverse side if necessary and identify by block number)

Photoelectron spectroscopy, shakeup, nitrogen, photodissociation

20 ABSTRACT (Continue on reverse side if necessary and identify by block number)

The inner-valence (20-36eV) photoelectron spectrum of N_2 is interpreted by comparing with various spectra (such as absorption, N_2^+ yield, fluorescence-yield, and core-level photoelectron spectra) and with previously published theoretical calculations.

This empirical interpretation allows for unique assignments, and enables us to distinguish between the four previously published theoretical calculations which lead to inconsistent assignments.

DD FORM 1 JAN 73 1473 EDITION OF 1 NOV 65 IS OBSOLETE S/N 0102-014-6601

Unclassified

SECURITY CLASSIFICATION OF THIS PAGE (When Data Entered)

DTIC FILE COPY

AD-A162 103

(12)

OFFICE OF NAVAL RESEARCH

N00014-80-K-0852

Task No. 056-681

Technical Report No. 21

AN INTERPRETATION OF THE N_2 PHOTOELECTRON SPECTRUM

By

Hideo Sambe and David E. Ramaker

Prepared for Publication

in

Chemical Physics Letters

George Washington University
Department of Chemistry
Washington D.C. 20052

October 1985

DISCLAIMER NOTICE

THIS DOCUMENT IS BEST QUALITY PRACTICABLE. THE COPY FURNISHED TO DTIC CONTAINED A SIGNIFICANT NUMBER OF PAGES WHICH DO NOT REPRODUCE LEGIBLY.

An Interpretation of the N_2 photoelectron Spectrum**

Hideo Sambe and David E. Ramaker

Chemistry Department, George Washington University

Washington, DC 20052, USA

** Supported by the Office of Naval Research

Abstract

The inner-valence (20-36eV) photoelectron spectrum of N_2 is interpreted by comparing with various spectra (such as absorption, N^+-yield, fluorescence-yield, and core-level photoelectron spectra) and with theoretical calculations. The bands at 25.3, 29.0, 32.6, 33.4(sharp and weak), and 35eV(weak) are attributed to the $^2\Sigma_u^+(3\sigma_g^{-1}1\pi_u^{-1}1\pi_g)$, $^2\Sigma_g^+(2\sigma_u^{-1}1\pi_u^{-1}1\pi_g)$, $^2\Sigma_u^+(3\sigma_g^{-1}1\pi_u^{-1}1\pi_g)$, $^2\Pi_u(3\sigma_g^{-1}2\sigma_u^{-1}1\pi_g)$, and $^2\Sigma_g^+(3\sigma_g^{-1}1\pi_u^{2}1\pi_g^{2})$ states, respectively.

1. Introduction

The photoelectron spectrum (PES) by Nyholm et al. [1], the lower spectrum in Figure 1, clearly shows four bands around 25eV(C), 29eV(F), 33eV(E), and 38eV(H), and probably a weak band around 35eV(G). The recent measurement by Krummacher et al. [2], the upper spectrum in Figure 1, confirms the presence of these bands. H band, the strongest and broadest band among the five bands, is known to consist of several $^2\Sigma_g^+$ states that borrow their intensities from $2\sigma_g^{-1}$ configuration. In this letter, we assign symmetries and dominant *electronic configurations* to the C, F, E, and G bands.

First, we obtain symmetries and dominant configurations from experiments by comparing the PES with other spectra, such as the absorption spectrum, the N^+ yield spectrum, the core-level PES, and a valence-level PES of a different photon energy. Then, we compare the obtained symmetries and configurations with published theoretical calculations.

2. Observed Rydberg states and the inversion symmetry of its ion-core state.

There is a close relationship between an observed (that is, dipole-allowed) Rydberg state and the inversion symmetry of its ion-core state. Rydberg states that are excited from the N_2 ground state, $^1\Sigma_g^+$, by dipole transitions should have "u" symmetry because the dipole operator has "u" symmetry.

If a Rydberg state I-ns or I-nd is observed, its ion-core state I should have "u" symmetry because Rydberg orbital ns or nd has "g" symmetry. If a Rydberg state I-np is observed, its ion-core state I should have "g" symmetry because Rydberg orbital np has "u" symmetry.

Figure 2 shows how we identify the C-3d, F-3p, F-4p, and E-3s Rydberg states in the absorption (ABS) and N^+-yield spectra. The solid bars in the middle of the figure denote the Rydberg-electron binding energies that are estimated from the Rydberg states converging to the one-hole (1h) states. Note that the band widths of the C and C-3d states are similar and that those of the F and F-3p states are also similar. Paired vibrational progressions are identified for the C-3d state. Details of this identification will be published elsewhere.

The observation of the C-3d, F-3p (or F-4p), and E-3s Rydberg states implies that the C, F, and E ionized states have "u", "g", and "u" symmetries, respectively.

3. Photon-energy variation of PES

Ionization into two-hole, one-electron (2h-1e) states or three-hole, two-electron (3h-2e) states is forbidden, because it involves a two- or three-electron-jump transition. 2h-1e or 3h-2e states gain their intensity through configuration-interaction (CI) mixing with 1h states. In a configuration interaction, only the states

that have the same symmetry can mix with each other. Therefore, the bands that are clearly observed in PES (such as the C, F, E, and G bands) should have either $^2\Sigma_g^+$ (the symmetry of the $2\sigma_g^{-1}$ and $3\sigma_g^{-1}$ states), $^2\Sigma_u^+$ (the symmetry of the $2\sigma_u^{-1}$ state), or $^2\Pi_u$ (the symmetry of the $1\pi_u^{-1}$ state).

Figure 1 compares PES s of different photon energies. When the photon energy is decreased from 1487eV to 50.3eV, the $3\sigma_g^{-1}$ and $1\pi_u^{-1}$ intensities increase relative to the $2\sigma_u^{-1}$ intensity and also the F intensity increases relative to the C, E, G, and H intensities. These relative increases are depicted by shaded areas in the figure. The simultaneous increases of the $3\sigma_g^{-1}$, $1\pi_u^{-1}$, and F intensities suggest that the F state mixes with either the $3\sigma_g^{-1}$ or $1\pi_u^{-1}$ state and also that the C, E, and G states do not mix with these states (that is, the C, E, and G states mix with either the $2\sigma_g^{-1}$ or $2\sigma_u^{-1}$ state).

In the preceding section, we have concluded that the F state should have "g" symmetry. Combining this and the above conclusion that the F state must mix with either the $3\sigma_g^{-1}$ or $1\pi_u^{-1}$ state, we conclude that the F state mixes with the $3\sigma_g^{-1}$ and $2\sigma_g^{-1}$ states. Since the C and E states should have "u" symmetry and must mix with either the $2\sigma_g^{-1}$ or $2\sigma_u^{-1}$ states, we conclude that the C and E states mix with the $2\sigma_u^{-1}$ state. In summary, the F state has the $^2\Sigma_g^+$

symmetry; the C and E states have the $^2\Sigma_u^+$ symmetry; and the G state has the $^2\Sigma^+$ symmetry.

4. The $^2\Sigma^+(no^{-1}1\pi_u^{-1}1\pi_g)$ shake-up states

The $no^{-1}1\pi_u\ ^1 1\pi_g$ configuration gives two $^2\Sigma^+$ states. We expect that their energies relative to the $^2\Sigma^+(no^{-1})$ state (that is, the $^2\Sigma^+(no^{-1}1\pi_u\ ^1 1\pi_g)$-$^2\Sigma^+(no^{-1})$ energies) are approximately independent of the no^{-1} hole. Here, the no^{-1} hole may be $1o^{-1}$, $2o_u^{-1}$, or $3o_g^{-1}$. The following analysis is based on this assumption.

The $^2\Sigma^+(1o^{-1}1\pi_u\ ^1 1\pi_g)$ states have been identified as the lowest two shake-up peaks in the core-level PES (the middle and bottom spectra of Figure 3) [3]. The second-lowest, shake-up peak is much stronger than the lowest shake-up peak, as seen in Figure 3, indicating that the higher $^2\Sigma^+(1o^{-1}1\pi_u\ ^1 1\pi_g)$ state mixes more strongly with the $^2\Sigma^+(1o^{-1})$ state.

When the $1o^{-1}$ peak of the core-level PES (the middle) is aligned with the $3o_g^{-1}$ peak of the valence-level PES (the top), the $^2\Sigma^+(1o^{-1}1\pi_u^{-1}1\pi_g)$ shake-up peaks nearly align with the C and E bands, as shown in the figure. This agreement suggests that the C and E bands are the $^2\Sigma_u^+(3o_g^{-1}1\pi_u^{-1}1\pi_g)$ shake-up states from the $3o_g^{-1}$ hole. In the preceding section, we have concluded that the C and E bands should have the $^2\Sigma_u^+$ symmetry. This conclusion confirms the above

statement. In summary, the C and E bands should have the $^2\Sigma_u^+$ symmetry and the $3\sigma_g^{-1}1\pi_u^{-1}1\pi_g$ configuration.

When the $1\sigma^{-1}$ peak of the core-level PES (the bottom) is aligned with the $2\sigma_u^{-1}$ peak of the valence-level PES (the top), the $^2\Sigma^+(1\sigma^{-1}1\pi_u^{-1}1\pi_g)$ shake-up peaks nearly align with the F and G bands (see Figure 3). This agreement would suggest that the F and G bands are the $^2\Sigma_g^+(2\sigma_u^{-1}1\pi_u^{-1}1\pi_g)$ states of the $2\sigma_u^{-1}$ hole. However, the core-level PES also suggests that the G band should be stronger than the F band, contrary to Figure 3. We attribute the H' band, which is indicated in Figure 1, to the higher $^2\Sigma_g^+(2\sigma_u^{-1}1\pi_u^{-1}1\pi_g)$ state. This assignment will be discussed elsewhere. In the preceding section, we concluded that the F band should have the $^2\Sigma_g^+$ symmetry. This conclusion confirms the $^2\Sigma_g^+(2\sigma_u^{-1}1\pi_u^{-1}1\pi_g)$ assignment of the F band.

5. Band widths of PES

Based on their bonding ($3\sigma_g$ and $1\pi_u$) and antibonding ($2\sigma_u$ and $1\pi_g$) characters, we expect that the FWHM s of the two $^2\Sigma_u^+(3\sigma_g^{-1}1\pi_u^{-1}1\pi_g)$ states are similar to each other and are larger than the FWHM s of the $^2\Sigma_g^+(2\sigma_u^{-1}1\pi_u^{-1}1\pi_g)$ states. Schirmer et al. [4] calculated the FWHM s for these states and confirmed the above expectation: 2.06eV and 2.12eV for the $^2\Sigma_u^+(3\sigma_g^{-1}1\pi_u^{-1}1\pi_g)$ states and 1.24eV for the lower $^2\Sigma_g^+(2\sigma_u^{-1}1\pi_u^{-1}1\pi_g)$ state.

The observed FWHM's(≈2.2eV) of the C and E bands are similar to each other and are larger than the observed FWHM(≈ 1.6eV) of the F band. These observed band widths support the C $^2\Sigma_u^+(3\sigma_g^{-1}1\pi_u^{-1}1\pi_g)$, E $^2\Sigma_u^+(3\sigma_g^{-1}1\pi_u^{-1}1\pi_g)$, and F $^2\Sigma_g^+(2\sigma_u^{-1}1\pi_u^{-1}1\pi_g)$ assignments. The C $^2\Sigma_u^+(3\sigma_g^{-1}1\pi_u^{-1}1\pi_g)$ assignment has been well established through studies on the C—X transition [5,6].

b. Theoretical calculations

Figure 4 compares the experimental results (the first column) with published theoretical calculations (the remaining columns). The shaded bars depict the band-peak energies from PES. The symmetries and the dominant configurations in the first column are those determined in the previous sections. The (+3) indicates the presence of both $2\sigma_g^{-1}$ and $3\sigma_g^{-1}$ mixing, and the (-3) indicates the absence of the $3\sigma_g^{-1}$ mixing.

Theoretical calculations shown are the lowest six states that have either $^2\Sigma_g^+$, $^2\Pi_u$, or $^2\Sigma_u^+$ symmetry, excluding the X $^2\Sigma_g^+(3\sigma_g^{-1})$, A $^2\Pi_u(1\pi_u^{-1})$ and B $^2\Sigma_u^+(2\sigma_u^{-1})$ states. Solid bars show the calculated vertical ionization potentials, and the numbers above or below the bars give the one-hole mixing intensities. The $^2\Sigma_g^+$ state mixes with two one-hole states, the $2\sigma_g^{-1}$ and $3\sigma_g^{-1}$ states; the upper number denotes the $2\sigma_g^{-1}$ mixing intensity. The symmetries and the dominant configurations in the last column are determined from calculations.

The computational methods used were the partitioning CI (Kosugi et al. [7]), the polarization CI (Langhoff et al. [8]), the multiconfigurational Green's function (Nichols et al. [9]), and the equation-of-motion Green's function (Herman et al. [10]). Kosugi's, Langhoff's and Nichols' calculations include the 1h, 2h-1e, and 3h-2e configurations, but Herman's calculation includes only the 1h and 2h-1e configurations. Calculations that are not shown in Figure 4, such as those by Schirmer et al. [4,11], and the single-excitation CI and 2ph-TDA Green's function calculations in Ref. [8], also include only the 1h and 2h-1e configurations and give results similar to Herman's calculation. It has been demonstrated [7,8] that the inclusion of the 3h-2e configurations is essential to provide accuracy for the higher states above 32eV.

For the C and F bands, the theoretical calculations almost reproduce the experimental results for the band energies, the band intensities, the symmetries, and the dominant electronic configurations. The theoretical calculations except Nichols' calculation agree on the amount of $3\sigma_g^{-1}$ mixing in the F state. The calculated intensity for the $^2\Pi_u$ state around 28eV is too weak to be observed.

For the E band, Kosugi's and Langhoff's calculations agree with the experimental results for the band energies, the band intensities, the symmetries, and the dominant electronic configuration. Note that the calculated

intensity for the $^2\Pi_u$ state around 33eV is too weak to assign to the E band.

For the G band, the theoretical calculations agree with the experimental results for the band energy, band intensity, the symmetry, and the near absence of $3\sigma_g^{-1}$ mixing. The theoretical dominant configuration $3\sigma_g^{-1}1\pi_u^{-2}1\pi_g^2$ is also consistent with the experimental evidence that $2\sigma_u^{-1}1\pi_u^{-1}1\pi_g$ is not a dominant configuration. Based on this agreement, we assign the $^2\Sigma_g^+(3\sigma_g^{-1}1\pi_u^{-2}1\pi_g^2)$ state to the G band.

The above comparisons suggest that Kosugi's and Langhoff's calculations are reliable. These two calculations predict a low-intensity $^2\Pi_u(3\sigma_g^{-1}2\sigma_u^{-1}1\pi_g)$ band around 33eV. This band is expected to be sharper than the F band (judging from its configuration) and to show the photon-energy variation similar to that of the F band (see Fig. 1). In Figure 2 of Reference [2], we can recognize a sharp low-intensity band at 33.3eV, which seems to show the expected photon-energy variation. Furthermore, a 31.5eV peak in the fluorescence spectrum [12] can be attributed to the 3d or 4s Rydberg state converging to this ionized state at 33.3eV. Based on these evidence, we identify the sharp low-intensity band at 33.3eV in the PES as the $^2\Pi_u(3\sigma_g^{-1}2\sigma_u^{-1}1\pi_g)$ state.

References

[1] R. Nyholm, A. Berndtsson, R. Nilsson, J. Hedman, and C. Nordling, Physica Scripta. 16(1977)383.

[2] S. Krummacher, V. Schmidt, and F. Wuilleumier, J. Phys. B 13(1980)3993.

[3] H. J. Freud, E. W. Plummer, W. R. Salaneck, and R. W. Bigelow, J. Chem. Phys. 75(1981)4275.

[4] J. Schirmer, L. S. Cederbaum, W. Domcke, and W. Von Niessen, Chem. Phys. 26(1977)149.

[5] K. P. Huber and G. Herzberg, "Molecular Spectra and Molecular Structure, IV Constants of Diatomic Molecules" (Van Nostrand Reinhold Co., New York, 1979).

[6] K. C. Joshi, Proc. Phys. Soc. 87(1966)285.

[7] N. Kosugi, H. Kuroda, and S. Iwata, Chem. Phys. 39(1979)337.

[8] P. W. Langhoff, S. R. Langhoff, T. N. Rescigno, J. Schirmer, L. S. Cederbaum, W. Domcke, and W. Von Niessen, Chem. Phys. 58(1981)71.

[9] J. A. Nichols, D. L. Yeager, and P. Jorgensen, J. Chem. Phys. 80(1984)293.

[10] M. F. Herman, K. F. Freed, and D. L. Yeager, Chem. Phys. 32(1978)437.

[11] J. Schirmer and O. Walter, Chem. Phys. 78(1983)201.

[12] L. C. Lee, R. W. Carlson, D. L. Judge, and M. Ogawa, J. Chem. Phys. 61(1974)3261.

Figure Captions

Fig. 1. Comparison of photoelectron spectra taken at two different incident photon energies. The shaded areas indicate the relative increase in the band intensities at the 50.3eV photon energy in comparison with those at the 1487eV photon energy.

Fig. 2. Indentification of the Rydberg states converging to the C, F, and E ionized states.

Fig. 3. The $^2\Sigma^+(n\sigma^{-1}1\pi_u^{-1}1\pi_g)$ shake-up states observed in the valence-level and core-level PES.

Fig. 4. Comparison of the experimental results with published theoretical calculations.

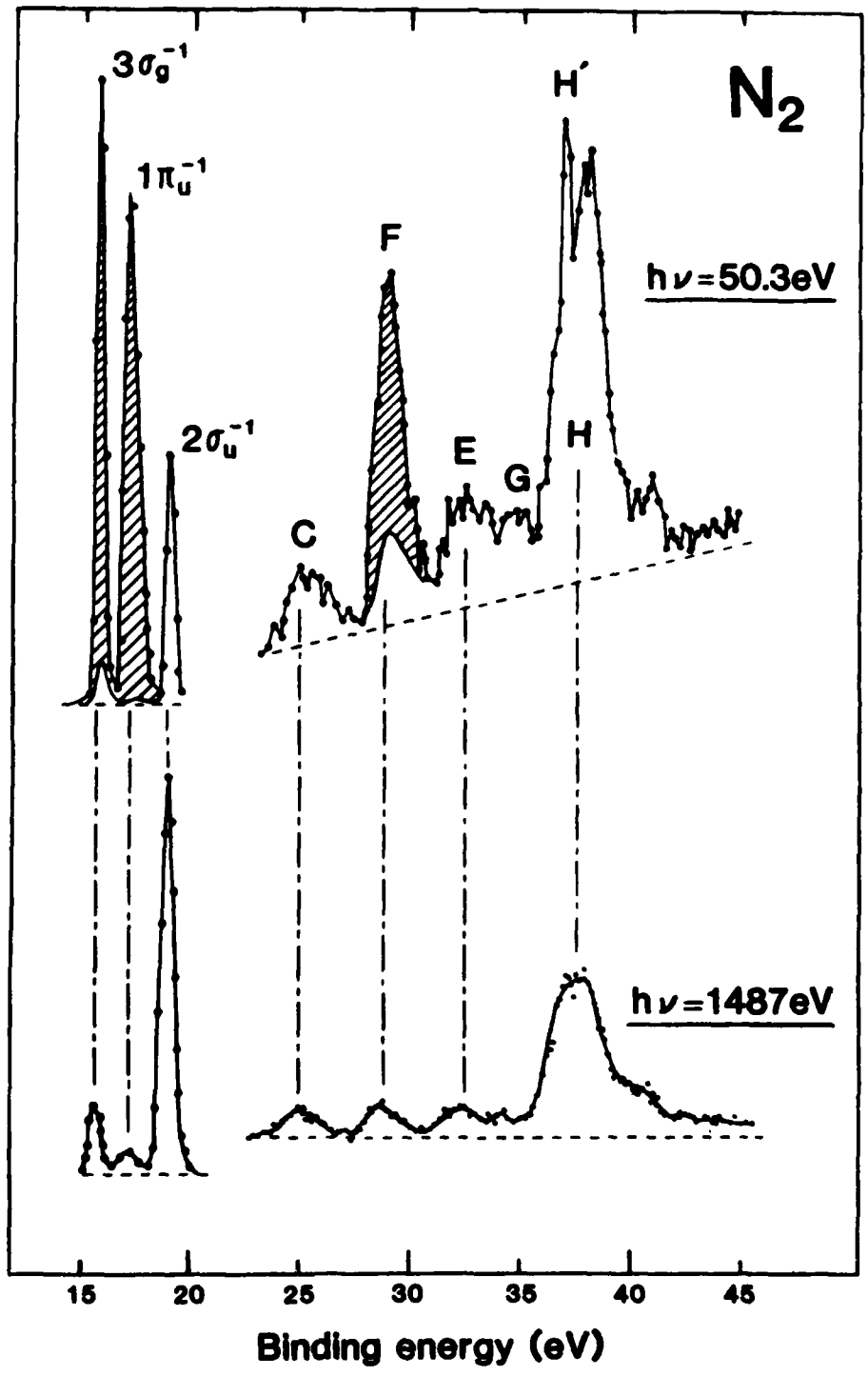
$3\sigma_g^{-1}$
$1\pi_u^{-1}$
$2\sigma_u^{-1}$
F
H'
N_2
$h\nu$=50.3eV
E
G
H
C
$h\nu$=1487eV
15
20
25
30
35
40
45
Binding energy (eV)

Fig. 1

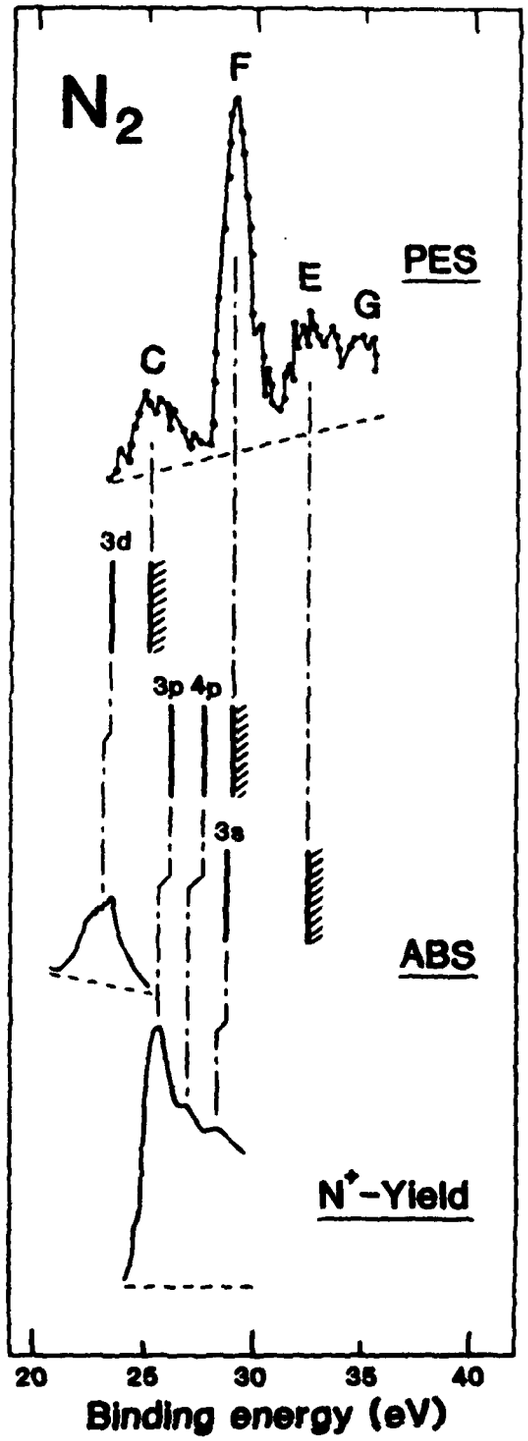
N2
F
E
G
C
PES
3d
3p 4p
3s
ABS
N+-Yield
20
25
30
35
40
Binding energy (eV)

Fig. 2

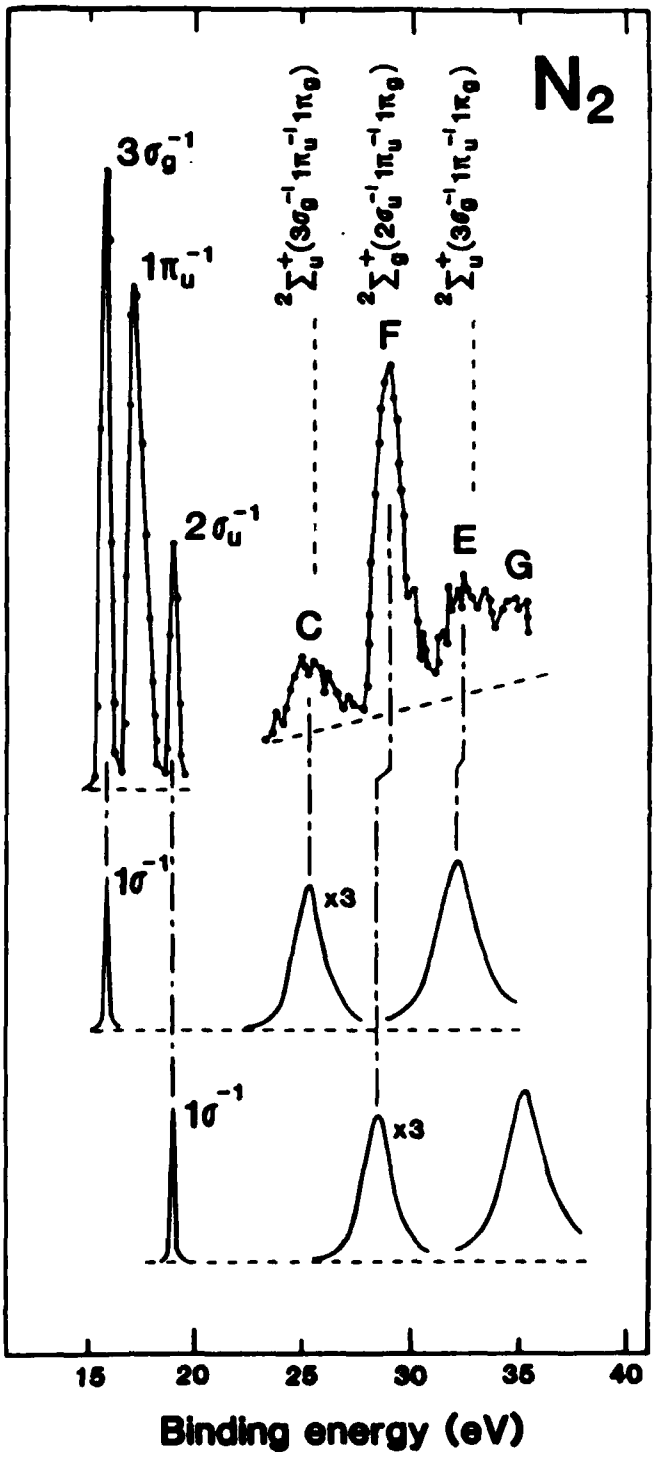
N2
3σg-1
1πu-1
2σu-1
1σ-1
1σ-1
2Σu+(3σg-1 1πu-1 1πg)
2Σg+(2σu-1 1πu-1 1πg)
2Σu+(3σg-1 1πu-1 1πg)
C
F
E
G
x3
x3
15
20
25
30
35
40
Binding energy (eV)

Fig. 3

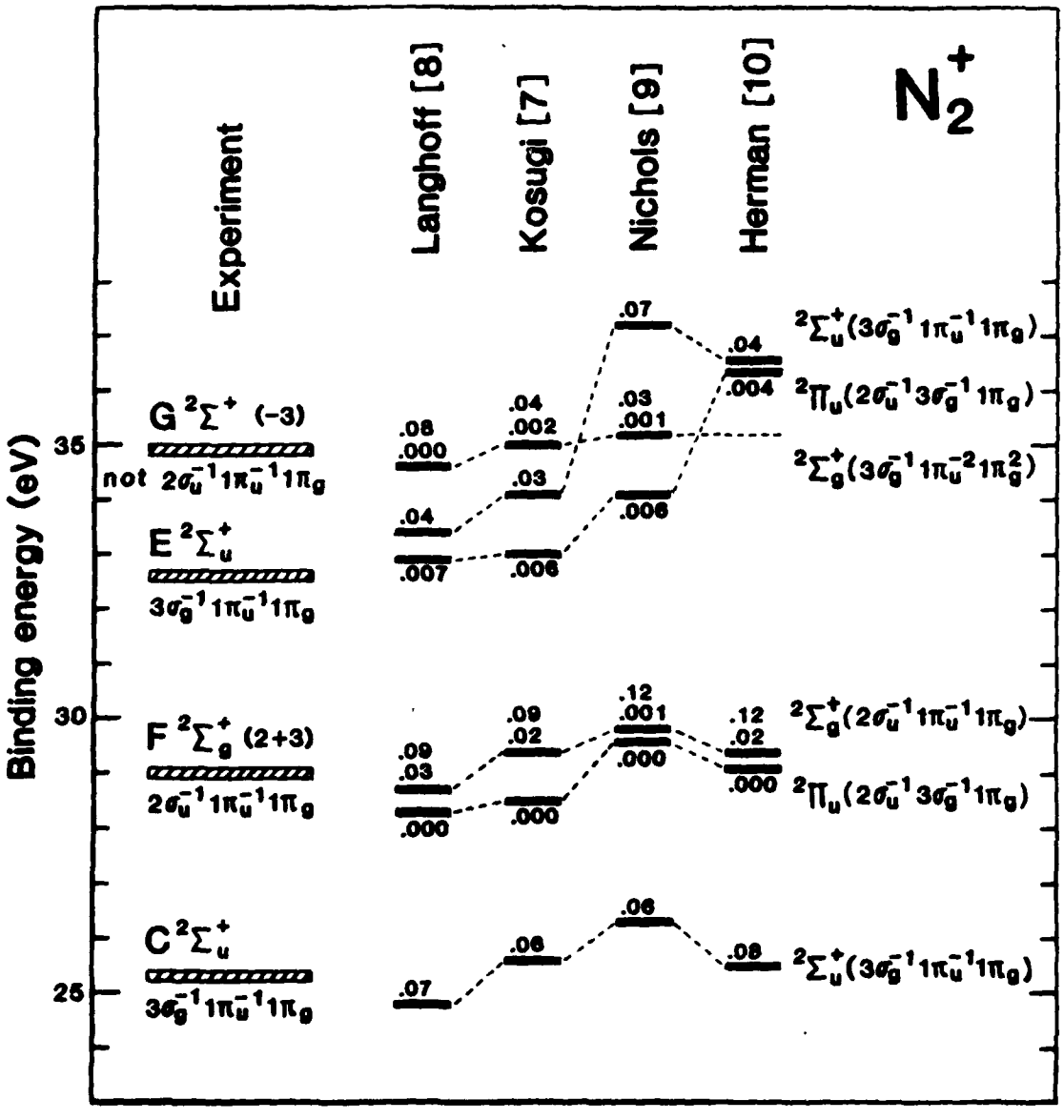
Experiment
Langhoff [8]
Kosugi [7]
Nichols [9]
Herman [10]
N_2^+
Binding energy (eV)
35
30
25
$G\,^2\Sigma^+$ (-3)
not $2\sigma_u^{-1}1\pi_u^{-1}1\pi_g$
$E\,^2\Sigma_u^+$
$3\sigma_g^{-1}1\pi_u^{-1}1\pi_g$
$F\,^2\Sigma_g^+$ (2+3)
$2\sigma_u^{-1}1\pi_u^{-1}1\pi_g$
$C\,^2\Sigma_u^+$
$3\sigma_g^{-1}1\pi_u^{-1}1\pi_g$
.08 .000
.04 .002
.07 .03 .001
.04
.03
.007 .006
.006
.09 .03 .000
.09 .02
.000
.12 .001 .000
.12 .02 .000
.07
.06
.08
.04 .004
$^2\Sigma_u^+(3\sigma_g^{-1}1\pi_u^{-1}1\pi_g)$
$^2\Pi_u(2\sigma_u^{-1}3\sigma_g^{-1}1\pi_g)$
$^2\Sigma_g^+(3\sigma_g^{-1}1\pi_u^{-2}1\pi_g^2)$
$^2\Sigma_g^+(2\sigma_u^{-1}1\pi_u^{-1}1\pi_g)$
$^2\Pi_u(2\sigma_u^{-1}3\sigma_g^{-1}1\pi_g)$
$^2\Sigma_u^+(3\sigma_g^{-1}1\pi_u^{-1}1\pi_g)$

Fig. 4

TECHNICAL REPORT DISTRIBUTION LIST, GEN

	No. Copies
Office of Naval Research Attn: Code 413 800 N. Quincy Street Arlington, Virginia 22217	2
Dr. Bernard Douda Naval Weapons Support Center Code 5042 Crane, Indiana 47522	1
Commander, Naval Air Systems Command Attn: Code 310C (H. Rosenwasser) Washington, D.C. 20360	1
Naval Civil Engineering Laboratory Attn: Dr. R. W. Drisko Port Hueneme, California 93401	1
Defense Technical Information Center Building 5, Cameron Station Alexandria, Virginia 22314	12
DTNSRDC Attn: Dr. G. Bosmajian Applied Chemistry Division Annapolis, Maryland 21401	1
Dr. William Tolles Superintendent Chemistry Division, Code 6100 Naval Research Laboratory Washington, D.C. 20375	1
Dr. David Young Code 334 NORDA NSTL, Mississippi 39529	1
Naval Weapons Center Attn: Dr. A. B. Amster Chemistry Division China Lake, California 93555	1
Scientific Advisor Commandant of the Marine Corps Code RD-1 Washington, D.C. 20380	1
U.S. Army Research Office Attn: CRD-AA-IP P.O. Box 12211 Research Triangle Park, NC 27709	1
Mr. John Boyle Materials Branch Naval Ship Engineering Center Philadelphia, Pennsylvania 19112	1
Naval Ocean Systems Center Attn: Dr. S. Yamamoto Marine Sciences Division San Diego, California 91232	1

ABSTRACTS DISTRIBUTION LIST, 056/625/629

Dr. F. Carter
Code 6132
Naval Research Laboratory
Washington, D.C. 20375

Dr. Richard Colton
Code 6112
Naval Research Laboratory
Washington, D.C. 20375

Dr. Dan Pierce
National Bureau of Standards
Optical Physics Division
Washington, D.C. 20234

Dr. R. Stanley Williams
Department of Chemistry
University of California
Los Angeles, California 90024

Dr. R. P. Messmer
Materials Characterization Lab.
General Electric Company
Schenectady, New York 22217

Dr. Robert Gomer
Department of Chemistry
James Franck Institute
5640 Ellis Avenue
Chicago, Illinois 60637

Dr. Ronald Lee
R301
Naval Surface Weapons Center
White Oak
Silver Spring, Maryland 20910

Dr. Paul Schoen
Code 5570
Naval Research Laboratory
Washington, D.C. 20375

Dr. John T. Yates
Department of Chemistry
University of Pittsburgh
Pittsburgh, Pennsylvania 15260

Dr. Richard Greene
Code 5230
Naval Research Laboratory
Washington, D.C. 20375

Dr. L. Kesmodel
Department of Physics
Indiana University
Bloomington, Indiana 47403

Dr. K. C. Janda
California Institute of Technology
Division of Chemistry and Chemical Engineering
Pasadena, California 91125

Dr. E. A. Irene
Department of Chemistry
University of North Carolina
Chapel Hill, Northc Carolina 27514

Dr. Adam Heller
Bell Laboratories
Murray Hill, New Jersey 07974

Dr. Martin Fleischmann
Department of Chemistry
Southampton University
Southampton SO9 5NH
Hampshire, England

Dr. John W. Wilkins
Cornell University
Laboratory of Atomic and Solid State Physics
Ithaca, New York 14853

Dr. Richard Smardzewski
Code 6130
Naval Research Laboratory
Washington, D.C. 20375

Dr. H. Tachikawa
Chemistry Department
Jackson State University
Jackson, Mississippi 39217

ABSTRACTS DISTRIBUTION LIST, 056/625/629

Dr. R. G. Wallis
Department of Physics
University of California
Irvine, California 92664

Dr. D. Ramaker
Chemistry Department
George Washington University
Washington, D.C. 20052

Dr. J. C. Hemminger
Chemistry Department
University of California
Irvine, California 92717

Dr. T. F. George
Chemistry Department
University of Rochester
Rochester, New York 14627

Dr. G. Rubloff
IBM
Thomas J. Watson Research Center
P.O. Box 218
Yorktown Heights, New York 10598

Dr. Horia Metiu
Chemistry Department
University of California
Santa Barbara, California 93106

Captain Lee Myers
AFOSR/NC
Bollig AFB
Washington, D.C. 20332

Dr. J. T. Keiser
Department of Chemistry
University of Richmond
Richmond, Virginia 23173

Dr. Roald Hoffmann
Department of Chemistry
Cornell University
Ithaca, New York 14853

Dr. J. E. Jensen
Hughes Research Laboratory
3011 Malibu Canyon Road
Malibu, California 90265

Dr. J. H. Weaver
Department of Chemical Engineering
and Materials Science
University of Minnesota
Minneapolis, Minnesota 55455

Dr. R. W. Plummer
Department of Physics
University of Pennsylvania
Philadelphia, Pennsylvania 19104

Dr. E. Yeager
Department of Chemistry
Case Western Reserve University
Cleveland, Ohio 41106

Dr. N. Winograd
Department of Chemistry
Pennsylvania State University
University Park, Pennsylvania 16802

Dr. G. D. Stein
Mechanical Engineering Department
Northwestern University
Evanston, Illinois 60201

Dr. A. Steckl
Department of Electrical and
Systems Engineering
Rensselaer Polytechnic Institute
Troy, NewYork 12181

Dr. G. H. Morrison
Department of Chemistry
Cornell University
Ithaca, New York 14853

Dr. P. Hansma
Physics Department
University of California
Santa Barbara, California 93106

Dr. J. Baldeschwieler
California Institute of Technology
Division of Chemistry
Pasadena, California 91125

Dr. W. Goddard
California Institute of Technology
Division of Chemistry
Pasadena, California 91125

Dr. W. Knauer
Hughes Research Laboratory
3011 Malibu Canyon Road
Malibu, California 90265

Dr. C. B. Harris
Department of Chemistry
University of California
Berkeley, California 94720

DL/413/83/01
056/413-2

ABSTRACTS DISTRIBUTION LIST, 056/625/629

Dr. G. A. Somorjai
Department of Chemistry
University of California
Berkeley, California 94720

Dr. J. Murday
Naval Research Laboratory
Surface Chemistry Division (6170)
155 Overlook Avenue, S.W.
Washington, D.C. 20375

Dr. J. B. Hudson
Materials Division
Rensselaer Polytechnic Institute
Troy, New York 12181

Dr. Theodore E. Madey
Surface Chemistry Section
Department of Commerce
National Bureau of Standards
Washington, D.C. 20234

Dr. J. E. Demuth
IBM Corporation
Thomas J. Watson Research Center
P.O. Box 218
Yorktown Heights, New York 10598

Dr. M. G. Lagally
Department of Metallurgical
and Mining Engineering
University of Wisconsin
Madison, Wisconsin 53706

Dr. R. P. Van Duyne
Chemistry Department
Northwestern University
Evanston, Illinois 60637

Dr. J. M. White
Department of Chemistry
University of Texas
Austin, Texas 78712

Dr. D. E. Harrison
Department of Physics
Naval Postgraduate School
Monterey, California 93940

Dr. W. Kohn
Department of Physics
University of California, San Diego
La Jolla, California 92037

Dr. R. L. Park
Director, Center of Materials
Research
University of Maryland
College Park, Maryland 20742

Dr. W. T. Peria
Electrical Engineering Department
University of Minnesota
Minneapolis, Minnesota 55455

Dr. Keith H. Johnson
Department of Metallurgy and
Materials Science
Massachusetts Institute of Technology
Cambridge, Massachusetts 02139

Dr. S. Sibener
Department of Chemistry
James Franck Institute
5640 Ellis Avenue
Chicago, Illinois 60637

Dr. Arold Green
Quantum Surface Dynamics Branch
Code 3817
Naval Weapons Center
China Lake, California 93555

Dr. A. Wold
Department of Chemistry
Brown University
Providence, Rhode Island 02912

Dr. S. L. Bernasek
Department of Chemistry
Princeton University
Princeton, New Jersey 08544

Dr. P. Lund
Department of Chemistry
Howard University
Washington, D.C. 20059

END

DATE
FILMED

-86

DTIC